Multistep Analysis of the Mechanical Performance of an Air Spring

Li Fengxiang, Ding Yumei, Yan Hua, Guan Changfeng, Yang Weimin

College of Mechanical and Electrical Engineering, Beijing University of Chemical Technology, Beijing 100029, People's Republic of China

Received 17 November 2007; accepted 15 July 2008
DOI 10.1002/app.29172
Published online 17 October 2008 in Wiley InterScience (www.interscience.wiley.com).

ABSTRACT: New methods for testing air springs have received a lot of interest in recent years. In this article APDL (ANSYS parametric design language) was utilized to simulate static and dynamic test process of air springs. In the simulation, multiple load steps solution was carried out through APDL *DO-LOOP and array parameter method. The program (capsule volume calculating macro) based on scatter sum method enabled the loop. The scalar quantity PRESSURE was established as inner tracking parameter to update inner pressure. Table parameter PRESSURES was established as inner pressure output parameter to export inner pressure of each load step. According to rubber elastic behavior and cord-rubber composite aeolotropy, hyper elastic element and layer element were preferred for simulation. Comparison was done between static simulation results and corresponding test data to prove feasibility of multistep analysis. In consequence, some major parameters such as cord angle, initial inner pressure, and auxiliary chamber volume were taken into account, which have remarkable effect on static mechanical performance of EQ6111 air spring. Finally, the same method was applied to the simulation of dynamic test process, achieving abundant analysis results according to every 0.5 Hz increment of load frequencies varying from 0.5 to 2.5 Hz. Load frequency threw remarkable effect on the dynamic mechanical performance of EQ6111 air spring, because inertial effect and damping effect played important roles therein. The study aims to make contribution to the development of platform of air spring simulation and parameterized design (PASSPD). J Appl Polym Sci 111: 1005–1012, 2009

Key words: air spring; multistep analysis; mechanical performance; rubber elastic behavior; cord-rubber composite aeolotropy

INTRODUCTION

Air spring is an important component used for vibration isolation. It has variable nonlinear static and dynamic stiffness and damping characteristics.[1] Free frequency of an air spring vibration isolation system hardly changes when load varies. This system can avoid resonance automatically, depressing resonance amplitude.[2] So air springs are widely used in automobile, mechanical instruments, marine, and aviation fields. Research of air spring makes great significance.[3,4] In recent years, research of air springs has received much interest. Considering the different point of concern, the author would like to take the study of air springs into three major fields, which are mechanical properties, applications, and control. Pesterev et al. advanced a novel approach to the calculation of pothole-induced contact forces in MDOF vehicle models, which contained an air spring for vibration isolation.[5] Lu[6] gave an optimum design of "road-friendly" vehicle suspension systems subjected to rough pavement surfaces and indicated that air suspension was a quite good alternative. Some other reports also revealed that air springs were widely applied to transportation area such as mobile agriculture machines[7] and trucks,[8] where air spring's performance played important roles. Michael and Amit[9] utilized passive and semi-active control strategies to design a neonatal transport unit for vibration isolation, while Shinji[10] adopted incline compensation control including an air-spring type active isolated apparatus. Singh et al.[11] investigated that air bending tool geometry could influence its product quality and mechanical performance, which may give some exciting implication of considering geometry of air springs. However, mechanical performance is the most essential characteristic of an air spring, which is the base of optimization design and various control methods. So study of mechanical performance of air springs is absolutely necessary and makes great significance. The technical scheme executed in the investigation was a combination of simulation and test. Test method and test data introduced in this article were provided by TMT (Zhuzhou Times New Materials Technology). ANSYS was utilized to simulate both

Correspondence to: L. Fengxiang (rujuhu@hotmail.com).

static and dynamic test process and comparison between test results and simulation results was presented. ANSYS is a general large-scale FEA (finite element analysis) program, which has a broad range of FEA functions from simple static analysis to complex nonlinear dynamic analysis.[12] ANSYS was proved to be suitable for simulation of air spring's test process. The main object of present investigation is simulation of the mechanical behavior of an automobile air spring EQ6111. The test method referred to was mainly evolved from GB/T 13061-91 Air Spring for Automotive Suspension-Rubber Bellows.

TEST METHOD AND DEVICE

Vertical static test

An inner pressure of P MPa was applied to the air spring system with auxiliary chamber volume of V L. Then air supply was cut off. A vertical displacement load of $\pm L$ mm was applied to the upper cover board (loading route is $0 \rightarrow -L$ mm$\rightarrow 0 \rightarrow L$ mm). Based on the very test data acquired above, the force–displacement curve, inner pressure–displacement curve, and effective bearing area–displacement curve were plotted. The pressure–stiffness curve was drawn by altering inner pressure and repeating the loading operation mentioned above while the auxiliary chamber volume–stiffness curve was achieved in the same way by varying auxiliary chamber volume instead.

Transverse static test

For the transverse static test, an inner pressure of P MPa was applied to the air spring system with auxiliary chamber volume of V L. As described in the previous case, air supply was then cut off, which was followed by the application of a transverse displacement load of $\pm L$ mm to the upper cover board (loading route is $0 \rightarrow -L$ mm$\rightarrow 0 \rightarrow L$ mm). Based on the test data acquired, the force–displacement curve, inner pressure–displacement curve, effective bearing area–displacement curve, inner pressure–stiffness curve, and auxiliary chamber volume–stiffness curve were plotted in the same way as that in the vertical static test.

Vertical and transverse dynamic test

An inner pressure of P MPa was applied to the air spring system with auxiliary chamber volume of V L. Then air supply was cut off. A vertical displacement load with amplitude of $\pm L$ mm and frequency of f Hz was applied to the upper cover board. Force–displacement curve, inner pressure–displacement curve, and effective bearing area–displacement curve were plotted. Inner pressure varied from 0.3 to 0.7 MPa, auxiliary chamber volume from 0 to 50 L, displacement load amplitude of 50 mm with frequencies varying from 0.5 to 2.5 Hz. Time effect, inertial effect, and damping effect were taken into account in dynamic test. Because loading course was important for dynamic test procedure. Air inside the capsule experienced an isolated process periodically, which differed from static ones.

In the transverse dynamic tests also force–displacement curve, inner pressure–displacement curve, and effective bearing area–displacement curve were made in a similar way as mentioned earlier in the vertical dynamic test. The only difference occurred in displacement load direction, which was switched to transverse orientation.

Test device

Test device for automobile air spring EQ6111 is shown in Figure 1, in which EQ6111's nether cover board was completely constrained. Displacement load was applied to the upper cover board to obtain various responses. The upper cover board was moved in the vertical and transverse direction to process vertical and transverse test, respectively. Sensor-based data acquisition system was employed

Figure 1 Test device for EQ6111 air spring.

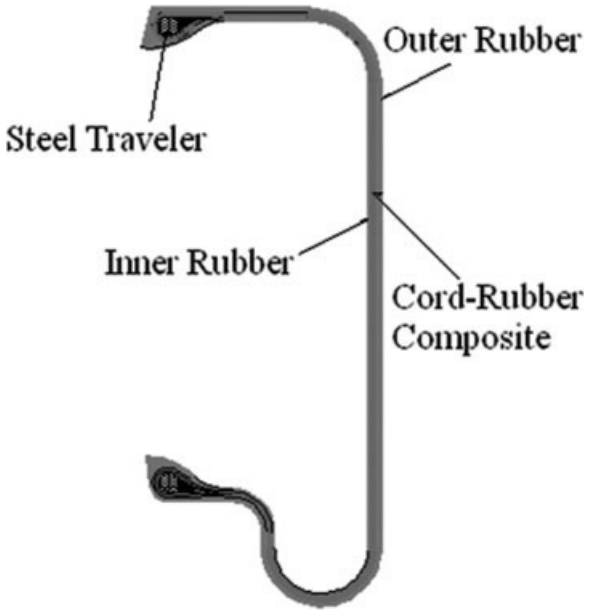

Figure 2 Capsule configuration of EQ6111 air spring.

to acquire, process displacement, and force signals which were then plotted versus true time. The test device was comprised of rack section, actuating mechanism, control system, and sensor-based data acquisition system to ensure both static and dynamic tests.

SIMULATION SCHEME

Structure and materials of EQ6111 air spring

EQ6111 air spring is mainly constructed of cover boards and capsule, in which capsule takes much greater part in air spring's mechanical performance. Figure 2 shows the configuration of EQ6111 air spring capsule. It is vulcanized from cord and rubber then mounted to cover boards through steel traveler. The outer rubber layer protects the capsule from general impairments, while the inner rubber layer is for pressure tightness. As the main body of the capsule, cord-rubber composite layers bear most of the forces applied to the air spring.

Phenomenological theory was adopted to describe rubber elastic behavior macroscopically, without taking into account microstructure of rubber. Phenomenological theory assumes that elastomers are isotropy, incompressible, and homogeneously deformed. Regarding rubber materials, the most universal function of strain energy density W was advanced by Rivlin as follows:

$$W = \sum_{i+j=1}^{N} C_{ij}(I_1 - 3)^i (I_2 - 3)^j \quad (1)$$

In which W is strain energy density, I_1 and I_2 are Green strain invariants, C_{ij} is material parameter.

Only taking first two items of eq. (1) into account, we can achieve Mooney-Rivlin constitutive equation:

$$W = C_1(I_1 - 3) + C_2(I_2 - 3) \quad (2)$$

In which C_1 and C_2 are material parameters. Based on simple extension, C_1 and C_2 were respectively, 0.36×10^6 and 0.1×10^6 in our research.

For orthotropic cord-rubber composite, thin-plate flexure theory was introduced to present its behavior based on certain assumptions. Stress and strain were considered to be vector sum of cord direction component and its normal direction component. Components of each direction correspondingly act only on cord or rubber. Magnitude of each component depends on composite cord angle. ANSYS Solid46 layer element was employed to reproduce the composite constitution through definition of real constant. Solid46 geometry was shown in Figure 3.

Multistep analysis

Simulation of air spring's test process was carried out under some presumptions and simplifications. Air in the capsule complicates simulation process. Although FSI (fluid-solid interaction) of ANSYS sustains analysis of this type, it has limitations to complexity and regularity of concerned structures. In this article, effect of air in the capsule was transformed into air pressure load applied on the inner wall of the capsule. During the loading course, air in the capsule obeys the Gas Equation:

$$PV^n = P_0V_0^n \quad (3)$$

In which P is inner pressure, V is capsule volume, P_0 is initial inner pressure, V_0 is initial capsule volume, n is polytropic exponent. In eq. (3), value of n depends on the loading course. n is set to be 1 in static course which is considered to be a constant temperature process, while it is 1.4 in dynamic course which is taken as an isolated process.

Process-dependency of air pressure load was one of the difficulties in simulation process. To solve the

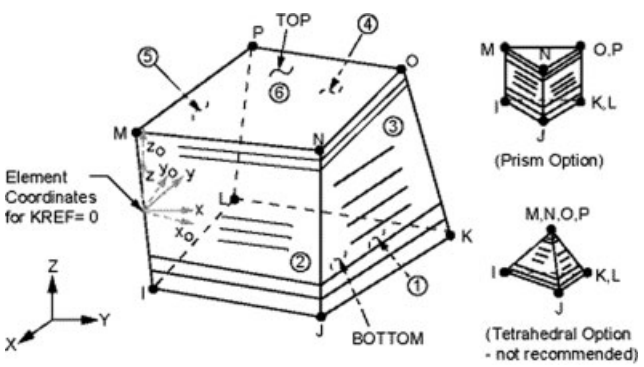

Figure 3 Solid46 layer element geometry.

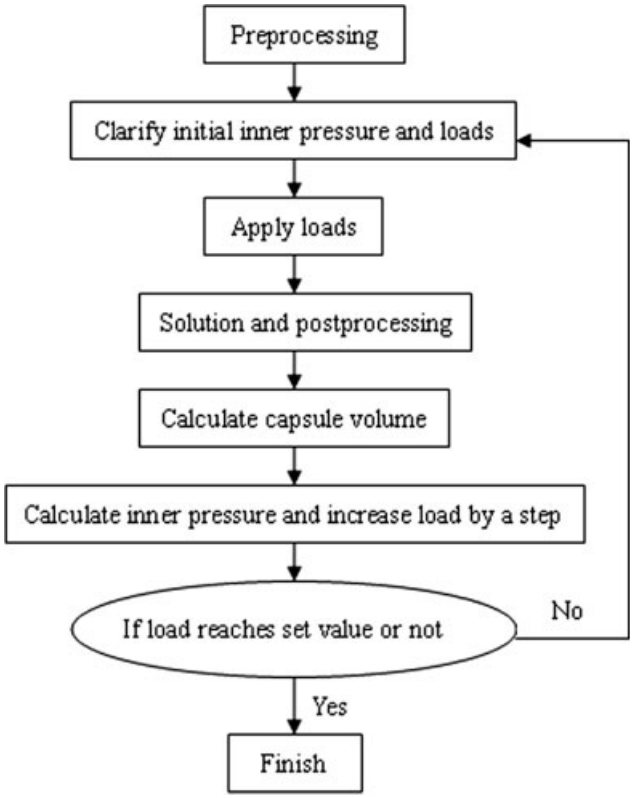

Figure 4 Flow chart of multistep analysis.

problem, multistep analysis was adopted, which was designed to disperse the loading course into fine enough steps. Multistep analysis was shown in Figure 4. Deformation of the capsule was tiny and inner pressure was considered to be constant in each step. The *DO-LOOP and array parameter method of APDL were utilized to launch multiple load steps solution.[13] Capsule volume V was calculated out by applying capsule volume calculating macro to deformed air spring. Then P was calculated through eq. (3) and assigned to inner pressure tracking parameter PRESSURE so as to update air pressure load. Meanwhile, displacement load increased by a step and went further to solution of the next load step.[14] Moreover, a table parameter PRESSURES was established as inner pressure output parameter in the loop to output inner pressure at the end of each load step.

Finite element model and loads

Elements were generated from nodes in ANSYS. Elements used were all low order ones. Steel traveler and cover boards were made of Solid45 elements. Inner and outer rubber layers were Hyper58 elements. Cord-rubber composite layers were comprised of Solid46 elements. The contact between capsule and cover boards was described with Targe170 and Conta173 elements.[15] Atmospheric pressure acted on capsule's outer wall where there

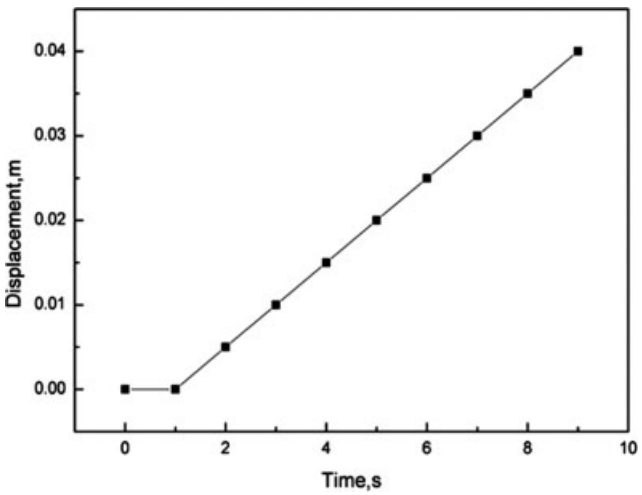

Figure 5 Displacement load course curve for static simulation.

was no contact. Inner pressure acted on capsule's inner wall. All DOFs (degree of freedom) of the nether cover board was restrained. Displacement load was applied to the upper cover board.

Displacement load applied to the upper cover board was comprised of two stages, pressure maintaining stage and load-on stage. Therefore, test simulation was divided into two corresponding stages. In the simulation, pressure maintaining stage simulation was carried out first through eq. (4) to work out gas equation constant C, which was indispensable for the APDL program of load-on stage simulation.

$$PV^n = P_0V_0^n = C \tag{4}$$

In this equation, P_0 is initial inner pressure, V_0 is initial capsule volume, n is polytropic exponent, C is gas equation constant. Figure 5 is a chart of displacement load course curve for static course and Figure 6 is a chart of displacement load course curve for

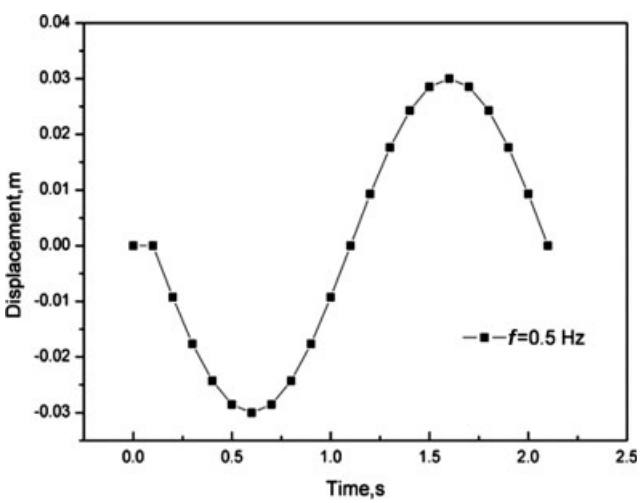

Figure 6 Displacement load course curve for dynamic simulation.

dynamic course. In the above-mentioned two figures, the horizontal part represents pressure maintaining stage, and the right parts denote load-on stage.

Capsule volume calculating macro and algorithm

The calculation of capsule volume is of great significance in multistep analysis of air springs. According to the finite element model mentioned above, capsule volume calculating macro was built upon scatter sum method, which was based on double integral algorithm.

When elements of the inner wall of the capsule were projected to a coordinate plane (*xoy* plane for example), capsule volume can be calculated as follows:

$$V = \int\int |z(x,y)|dxdy \tag{5}$$

In which V is capsule volume, $z = z(x,y)$ is the mathematical equation of the inner wall of the air spring.

In finite element analysis, the inner wall has been dispersed in ANSYS and coordinates of associated nodes can be got through NX(), NY(), and NZ() commands. So capsule volume eq. (5) can be transformed to be:

$$V = \Sigma V_i \tag{6}$$

where $V_i = |a_i \times h_i|$, a_i is the projection area of an element, h_i is the average distance between the element and the coordinate plane. According to triangle elements[14]:

$$h_i = \frac{1}{3} \times (z_{i1} + z_{i2} + z_{i3}) \tag{7}$$

$$a_i = \frac{1}{2} \times \begin{vmatrix} 1 & 1 & 1 \\ x_{i1} & x_{i2} & x_{i3} \\ y_{i1} & y_{i2} & y_{i3} \end{vmatrix} \tag{8}$$

For quadrangle elements:

$$h_i = \frac{1}{4} \times (z_{i1} + z_{i2} + z_{i3} + z_{i4}) \tag{9}$$

$$a_{i1} = \frac{1}{2} \times \begin{vmatrix} 1 & 1 & 1 \\ x_{i1} & x_{i2} & x_{i3} \\ y_{i1} & y_{i2} & y_{i3} \end{vmatrix} \tag{10}$$

$$a_{i2} = \frac{1}{2} \times \begin{vmatrix} 1 & 1 & 1 \\ x_{i1} & x_{i3} & x_{i4} \\ y_{i1} & y_{i3} & y_{i4} \end{vmatrix} \tag{11}$$

$$a_i = a_{i1} + a_{i2} \tag{12}$$

Capsule volume was eventually worked out through eq. (6). In the study, quadrangle elements were employed to discretize capsule. So, eqs. (9)–(12) were utilized for programming capsule volume calculating macro in ANSYS parametric design language. Capsule volume calculating macro based on scatter sum method can work out an accurate enough capsule volume as long as elements were fine enough. Therefore, capsule volume calculating macro was built upon the algorithm above, enabling the *DO-LOOP.

TABLE I
Simulation Results and Test Data of Inner Pressures

Displacement (mm)	Simulation (MPa)	Test (MPa)	Relative error (%)
−40	0.268657	0.2395	12.17411
−35	0.272035	0.2453	10.8989
−30	0.275556	0.2506	9.9585
−25	0.279075	0.2571	8.547258
−20	0.282871	0.2642	7.066995
−15	0.28642	0.2708	5.768095
−10	0.290884	0.2795	4.072987
−5	0.293783	0.2847	3.190376
0	0.3	0.2899	3.48396
5	0.306452	0.3001	2.116628
10	0.309566	0.3074	0.704619
15	0.314777	0.3143	0.151766
20	0.318939	0.3211	−0.673
25	0.323912	0.3313	−2.23
30	0.328554	0.3411	−3.6781
35	0.333659	0.3495	−4.53247
40	0.338579	0.3579	−5.39844

FEASIBILITY EVALUATION OF MULTISTEP ANALYSIS

Vertical static test simulation was launched in terms of the simulation scheme discussed above with initial inner pressure of 0.3 MPa, cord angle of 65°, auxiliary chamber volume of 0 L. Simulation results and test results were compared. Comparison of inner pressure was shown in Table I, while reaction force was shown in Table II. To make it clearer, test results of reaction force concerned with different initial inner pressures were also shown in Figure 7.

Simulation results approached the test results very well. The comparison showed that simulation could satisfy required precision. Multistep analysis was proved to be feasible. Further work would be done by altering initial inner pressure, cord angle, and auxiliary chamber volume to review the effect of these major parameters on air spring's static mechanical performance.

STATIC SIMULATION

Based on the simulation scheme given above, further static simulation was done according to different

TABLE II
Simulation Results and Test Data of Reaction Forces

Displacement (mm)	Simulation (KN)	Test (KN)	Relative error (%)
−40	11.97473	12.4449	−3.77801
−35	12.30529	12.7753	−3.67905
−30	12.6343	13.0396	−3.10822
−25	12.98131	13.2599	−2.101
−20	13.32236	13.4141	−0.68391
−15	13.70859	13.6344	0.544138
−10	14.02258	13.8326	1.373422
−5	14.502	14.0529	3.195782
0	14.69794	14.1851	3.615343
5	14.89562	14.4052	3.404465
10	15.37564	14.6035	5.287363
15	15.72014	14.7577	6.521612
20	16.1489	14.9339	8.135852
25	16.52965	15.2632	8.297408
30	16.94095	15.6141	8.497768
35	17.34468	15.9649	8.642585
40	17.75604	16.3157	8.827939

initial inner pressures, cord angles, and auxiliary chamber volumes, which are the major implicit factors that determine air spring's static mechanical performance.

Effect of initial inner pressure

Initial inner pressure played an important part in air spring's static mechanical performance. Both transverse static stiffness and vertical static stiffness increased with the accretion of initial inner pressure as shown in Figures 7 and 9, where cord angle was 65°, auxiliary chamber volume was 0 L. Figures 7 and 9 can be explained that air compression makes remarkable contribution both to air spring's transverse static stiffness and vertical static stiffness.

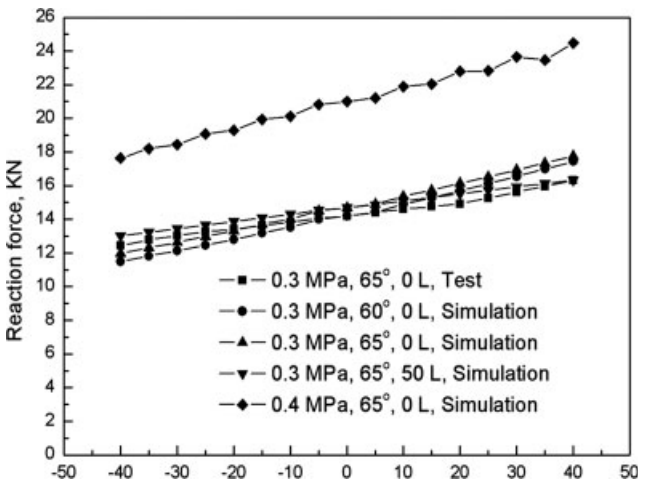

Figure 7 Static vertical force–displacement curve.

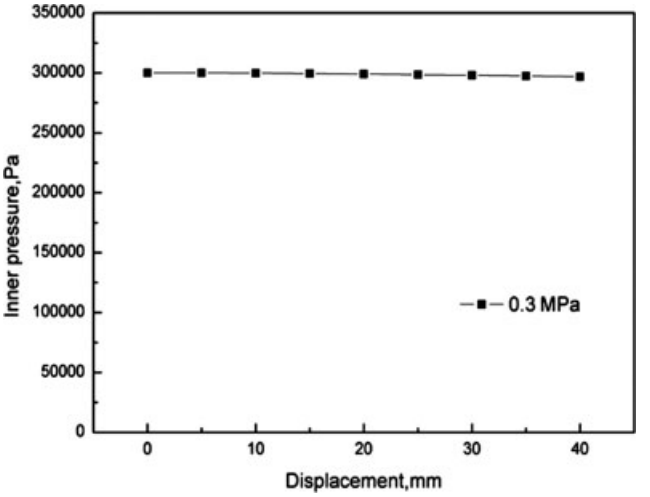

Figure 8 Variation of inner pressure in transverse simulation.

Effect of cord angle

Cord angle threw much more obvious effect on transverse static stiffness than vertical static stiffness, though they both rose with the increment of cord angle.[16] Effect of cord angle on transverse and vertical static mechanical performance were shown in Figures 7 and 9, where initial inner pressure was 0.3 MPa, auxiliary chamber volume was 0 L. It is believed that cord orientation directly affects stress and strain distribution in cord-rubber composite, further influencing air spring's transverse static stiffness and vertical static stiffness.

Effect of auxiliary chamber volume

Capsule volume used is assumed to be constant during the loading course of transverse test. In other words, inner pressure hardly changed during the transverse loading course.[17,18] This assumption was clarified by Figure 8. Auxiliary chamber volume is an addition to capsule volume. Air spring's capsule is nearly isovolumetric during transverse deformation while it is compressed or released during vertical deformation. Auxiliary chamber volume hardly threw any effect on air spring's transverse static stiffness while it obviously enhanced the linearity of static vertical force–displacement curve and weakened the nonlinearity of stiffness as respectively, shown in Figures 7 and 9. Air spring's vertical static stiffness decreased with the increment of auxiliary chamber volume. In Figures 7 and 9, initial inner pressure was set to be 0.3 MPa and cord angle was 65°.

DYNAMIC SIMULATION

Loop-line numeration of dynamic stiffness

Air spring's dynamic stiffness is defined in a quite different way. Under vibration with certain frequency

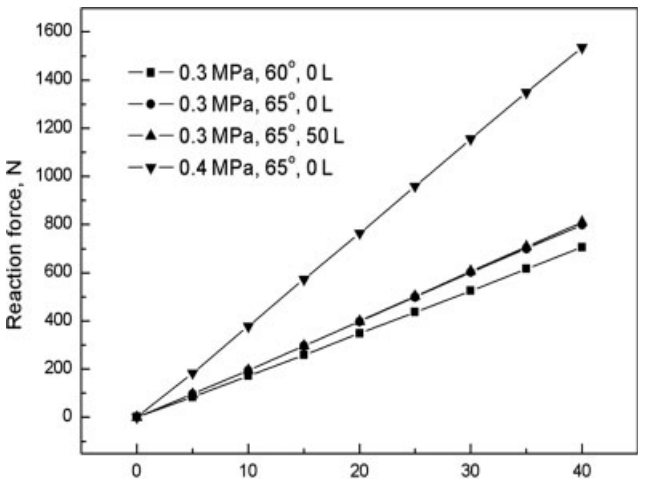

Figure 9 Static transverse force–displacement curve.

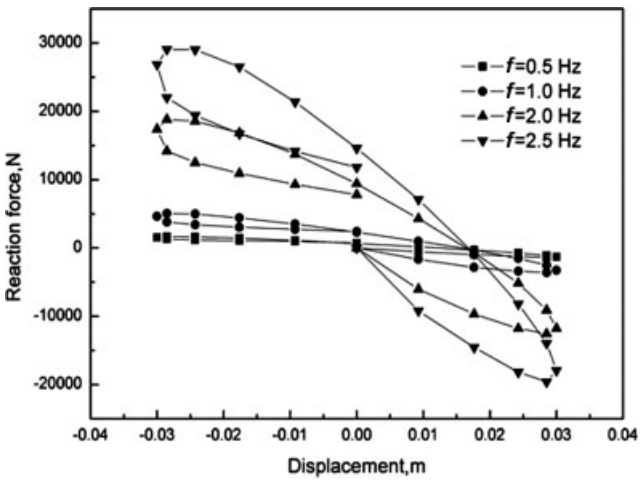

Figure 11 Dynamic transverse force–displacement curve.

and amplitude, the complex number ratio between air spring's load and displacement is defined to be its dynamic stiffness. An air springs' dynamic load–displacement curve is shown in Figure 10, in which dynamic stiffness can be calculated according to loop-line numeration method as follows[19]:

$$K_d = \frac{2P_0}{2X_0}\sqrt{1 - \left(\frac{\overline{JJ}'}{2P_0}\right)^2} \tag{13}$$

In eq. (13) K_d is air spring's dynamic stiffness, $2P_0$ is load span, $2X_0$ is maximum displacement, $\overline{JJ}'$ is the load difference when displacement is zero. Lost dynamic stiffness is calculated in terms of:

$$K'_d = \frac{\overline{JJ}'}{2X_0} \tag{14}$$

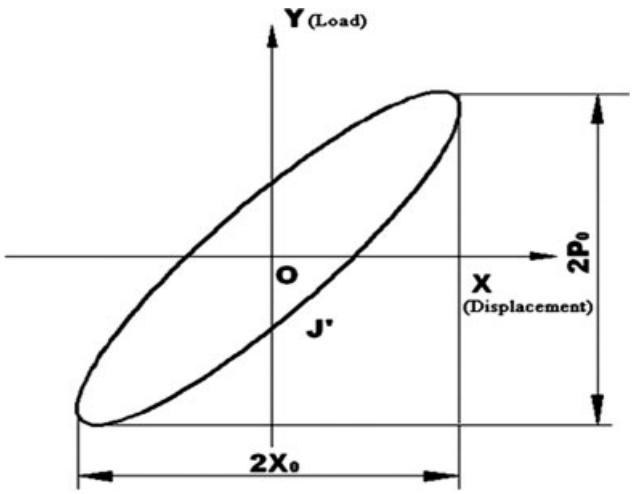

Figure 10 Dynamic load–displacement curve of an air spring.

Simulation results

Based on the simulation scheme above, further dynamic simulation was done according to every 0.5 Hz increment of load frequencies varying from 0.5 to 2.5 Hz, which is a major explicit factor that affects air spring's dynamic mechanical performance.[20] Figures 11 and 12 clearly show that displacement load frequency has a remarkable effect on transverse and vertical dynamic mechanical performance of EQ6111 air spring. The force rings expand with increment of load frequency as shown in Figures 11 and 12, indicating that both transverse and vertical dynamic stiffness increase with load frequency rising. The reason is that stress rigidization plays much more important role at higher load frequency.

CONCLUSIONS AND SIGNIFICANCES

Results of this article confirm that FEA simulation of air springs was feasible. Application of *DO-LOOP,

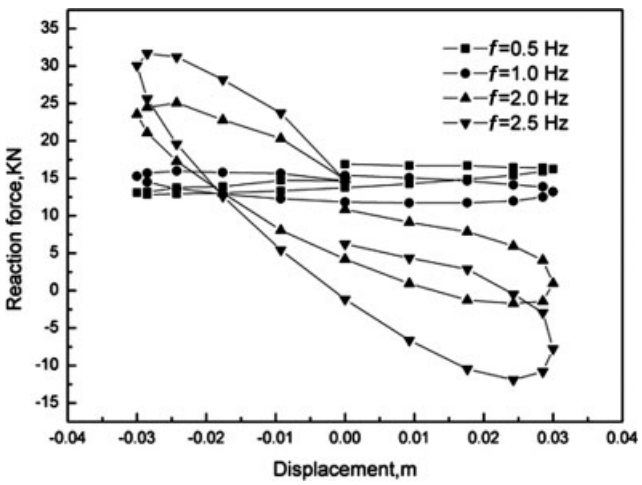

Figure 12 Dynamic vertical force–displacement curve.

capsule volume calculating macro, inner pressure tracking parameter, and inner pressure output parameter enabled the simulation to be done in succession. This is also an innovation of simulation research.

Simulation of static test displayed that initial inner pressure, cord angle, and auxiliary chamber volume play an important role in air spring's static vertical mechanical performance.[21] However, only initial inner pressure and cord angle revealed visible effect on its static transverse mechanical performance. Optimum design can be achieved by altering these major parameters. Dynamic simulation claimed that dynamic stiffness of air springs was quite sensitive to displacement load frequency. Much more data can be achieved by extending the technical scheme to simulation of every imaginable work condition of air springs to enrich analysis data base. Eventually, the study aims to make contribution to the development of platform of air spring simulation and parameterized design (PASSPD).

The authors thank Prof. Sabu Thomas from Mahatma Gandhi University for his kind advice and revision to the paper. The authors would also like to acknowledge Dr. Nishar Hameed for his kind guidance for submitting paper.

References

1. Lee, J. H.; Kim, K. J. J Sound Vib 2007, 301, 909.
2. Lou, J.; Zhu, S. Noise Vib Control 2001, 21, 22.
3. Kenji, K.; Tomonori, K.; Koichi, S.; Toshiharu, K. Precision Eng 2007, 31, 139.
4. Tomonori, K.; Kenji, K.; Koichi, S.; Toshiharu, K. Precision Eng 2007, 31, 269.
5. Pesterev, A. V.; Bergman, L. A.; Tan, C. A. J Sound Vib 2004, 275, 127.
6. Lu, S. Appl Math Model 2002, 26, 635.
7. Hostens, I.; Deprez, K.; Ramon, H. J Sound Vib 2004, 276, 141.
8. Jagjit S.; Paul Singh, S.; Eric, J. Packag Technol Sci 2006 19, 309.
9. Michael, B. V. K.; Amit, S. J Sound Vib 2005, 286, 382.
10. Shinji, W. Precision Eng 2003, 27, 170.
11. Singh, U. P.; Maiti, S. K.; Date, P. P.; Narasimhan, K. J Mater Process Technol 2004, 145, 269.
12. Ye, X.; Shi, Y. ANSYS Project Analysis Application Examples, 3rd ed.; Tsinghua University Press: Beijing, 2003.
13. Li, F.; Yang, W.; Ding, Y. J Syst Simul 2007, 19, 437.
14. Wu, S.; Huang, Y. J Nav Univ Eng 2001, 13, 94.
15. Yang, W.; Chen, C.; Chen, Y.; Ren, Y. J Beijing Univ Chem Technol 2004, 31, 105.
16. Zhu, D. Air Spring and Air Spring Control System, 1st ed.; Shandong Science and Technology Press: Jinan, 1989.
17. Mitsuru, K.; Tsutomu, I.; Katsuhiko, U.; Takahiro, S.; Satoshi, M. Transactions of the 17th International Conference on Structural Mechanics in Reactor Technology, Prague, 2003.
18. Ren, Y.; Yang, W. J Beijing Univ Chem Technol 2005, 32, 95.
19. Sun, W.; Liu, Y.; Chen, J. Automobile Technol 1999, 149, 1.
20. Katsuya, T.; Chuuji, Y.; Toshiharu, K.; Toshinori, F. JSAE Rev 1999, 20, 349.
21. Ouyang, Q.; Shi, Y. Mech Syst Signal Process 2003, 17, 705.